Cancer Letters 444 (2019) 45–59

Contents lists available at ScienceDirect

Cancer Letters

journal homepage: www.elsevier.com/locate/canlet

Original Articles

Rafoxanide, an organohalogen drug, triggers apoptosis and cell cycle arrest in multiple myeloma by enhancing DNA damage responses and suppressing the p38 MAPK pathway

Wenqin Xiao[a,1], Zhijian Xu[b,1], Shuaikang Chang[a,1], Bo Li[b], Dandan Yu[a], Huiqun Wu[a], Yongsheng Xie[a], Yingcong Wang[a], Bingqian Xie[a], Xi Sun[a], Yuanyuan Kong[a], Xiucai Lan[a], Wenxuan Bu[a], Gege Chen[a], Lu Gao[a], Xiaosong Wu[a], Jumei Shi[a,*], Weiliang Zhu[b,**]

[a] Department of Hematology, Shanghai Tenth People's Hospital, Tongji University School of Medicine, Shanghai, 200072, China
[b] CAS Key Laboratory of Receptor Research, Drug Discovery and Design Center, Shanghai Institute of Materia Medica, Chinese Academy of Sciences, Shanghai, 201203, China

ARTICLE INFO

Keywords:
Rafoxanide
Multiple myeloma
B-Raf
DNA damage
p38 MAPK pathway

ABSTRACT

Rafoxanide is used in veterinary medicine for the treatment of fascioliasis. We previously repositioned the drug as the inhibitor of B-Raf V600E, but its anti-tumor effect in human cancer has never been reported. In this study, we investigated the effects of rafoxanide in multiple myeloma (MM) *in vitro* and *in vivo*. We found that rafoxanide inhibited cell proliferation and overcame the protective effect of the bone marrow (BM) microenvironment on MM cells. Rafoxanide induced cell apoptosis by reducing mitochondrial membrane potential (MMP) and regulating the caspase pathway, while having no apparent toxic effect on normal cells. Rafoxanide also inhibited DNA synthesis and caused cell cycle arrest by regulating the cdc25A-degradation pathway. In addition, rafoxanide enhanced the DNA damage response by up-regulating the expression of γ-H2AX, and suppressed activation of the p38 MAPK pathway by down-regulating p38 MAPK phosphorylation and Stat1 phosphorylation. Rafoxanide treatment inhibited tumor growth, with no significant side effects, in an MM mouse xenograft model. Combination of rafoxanide with bortezomib or lenalidomide significantly induced synergistic cytotoxicity in MM cells. Finally, rafoxanide had anti-proliferation effect on both wild type and B-Raf V600E mutated MM cells. And the weaker anti-MM activity of rafoxanide than vemurafenib may indicate other potential mechanisms besides targeting B-Raf V600E mutation. Collectively, our results provide a rationale for use of this drug in MM treatment.

1. Introduction

Multiple myeloma (MM), a clonal plasma cell malignancy that accounts for approximately 10% of all hematological cancers, is associated with characteristic clinical complications, including skeletal destruction, renal impairment, anemia, and hypercalcemia [1,2]. Approximately 120,000 new cases of myeloma are diagnosed annually worldwide, an incidence rate that is expected to rise along with the aging world population [3]. Over the last few decades, proteasome inhibitors (bortezomib) and immunomodulatory drugs (thalidomide and lenalidomide) have greatly prolonged the survival of MM patients [4]. However, even though the prognosis of MM patients has

Abbreviations: MM, multiple myeloma; BM, bone marrow; MMP, mitochondrial membrane potential; MAPK, mitogen-activated protein kinase; ERK, extracellular signal-regulated kinase; BMSC, bone marrow stroma cells; BMMCs, bone marrow mononuclear cells; PBMCs, peripheral blood mononuclear cells; FBS, fetal bovine serum; CCK8, Cell Counting Kit-8; IL-6, interleukin-6; IGF-1, insulin-like growth factor-1; PI, propidium iodide; 7-AAD, 7-aminoactinomaycin D; EdU, 5-ethynyl- 2′-deoxyuridine; HE, hematoxylin and eosin; TUNEL, Terminal deoxynucleotidyl transferase dUTP nick end-labeling; IC_{50}, Half maximal inhibitory concentration; CI, combination index

* Corresponding author. Department of Hematology, Shanghai Tenth People's Hospital, Tongji University School of Medicine, 301 Yanchang Road, Shanghai, 200072, China.
** Corresponding author. CAS Key Laboratory of Receptor Research, Drug Discovery and Design Center, Shanghai Institute of Materia Medica, Chinese Academy of Sciences, 555 Zuchongzhi Road, Shanghai, 201203, China.
E-mail addresses: shijumei@tongji.edu.cn (J. Shi), wlzhu@simm.ac.cn (W. Zhu).
[1] These authors devoted equally to this study.

https://doi.org/10.1016/j.canlet.2018.12.014
Received 1 March 2018; Received in revised form 4 December 2018; Accepted 11 December 2018

significantly improved after the introduction of novel treatment agents, it remains incurable, with a high rate of relapse and refractory disease [5]. Thus, novel treatment agents with different mechanisms need to be identified.

Rafoxanide, *N*-[3-chloro-4-(4-chloro-phenoxy)phenyl]-2-hydroxy-3,5-diiodobenzamide, is an anthelmintic used in veterinary medicine for the treatment of fascioliasis in cattle and sheep [6]. Moreover, rafoxanide is also active against gastrointestinal nematodes and against nasal bot fly [7]. Matsubara et al. used an improved thyroid hormone reporter assay and found that rafoxanide has thyroid hormone-like activity [8]. Alamri et al. have shown that rafoxanide inhibits SPAK (STE20/SPS1-related proline/alanine-rich kinase) and OSR1 (oxidative-stress-responsive kinase 1) kinases [9]. Although rafoxanide has been used extensively in veterinary medicine, there is little information available concerning its biological effects on humans. However, a previous study reported the therapeutic use of rafoxanide in a child with fascioliasis, which is the first report in the literature concerning the usage of rafoxanide in humans [10]. Meanwhile, a recent study into the effects of rafoxanide on two human cell lines indicated that these veterinary anthelmintics have potential for the treatment of human disease [11]. With molecular docking and bioassay, we demonstrated that rafoxanide, an organohalogen drug, is a potent B-Raf V600E inhibitor [12].

Raf, a serine/threonine kinase, is a component of the mitogen-activated protein kinase (MAPK)/extracellular signal-regulated kinase (ERK) pathway, and it has attracted attention given the success of targeted therapy in many human cancer [13]. B-Raf has been found to be mutated in approximately 4% of MM cases, with the mutation of B-Raf V600E being the most common [14]. Although the B-Raf mutation is rare in MM, a case report showed that combination treatment with the small-molecular B-Raf V600E inhibitor vemurafenib and cobimetinib achieved a rapid and sustained response in a young patient with highly resistant and rapidly progressing MM haboring the B-raf V600E mutation [15]. The B-Raf V600E mutation causes constitutive activation of the Ras-Raf-MEK-ERK (RAS) and MAPK signaling pathway, further stimulating cell proliferation, differentiation and survival [16]. Therefore, in this study, we investigated the antitumor activities of rafoxanide in MM cell lines both *in vitro* and *in vivo*. Interestingly, we found that rafoxanide could induce significant cytotoxicity in MM cell lines *in vitro* and inhibit tumor growth in an MM mouse xenograft model *in vivo*. Furthermore, we examined the molecular mechanism of anti-MM activities induced by rafoxanide. In addition, we constructed B-Raf V600E overexpressed MM cells by lentivirus transduction, and B-Raf V600E knocked down MM cells by siRNA transduction to further explore the effect of rafoxanide.

2. Materials and methods

2.1. Cells and culture

H929, MM1S, U266 and BMSC line HS-5 were purchased from the American Type Culture Collection (ATCC) (Manassas, VA, USA). ARP1, OCI-MY5, OPM2 and RPMI8226 were kindly provided by Fenghuang Zhan (Department of Internal Medicine, University of Iowa, Iowa City, IA, USA). The bortezomib-resistant H929R was gained by our culture. HS-5 cells were stably transduced with GFP expressing lentivirus, which were kindly provided by professor Ping Wang (Tongji University School of Medicine, Shanghai, China). Primary cells were isolated from MM patient BM samples and peripheral blood of healthy donors using lymphoprep (Stemcell Technologies, Vancouver, BC, Canada) by Ficoll-Hypaque density gradient centrifugation. Then the bone marrow mononuclear cells (BMMCs) and peripheal blood mononuclear cells (PBMCs) were obtained. $CD138^+$ MM cells in BMMCs were then distinguished using the APC conjugated anti-CD138 (BioLegend, San Diego, CA, USA) according to the manufacturer's instructions. All primary samples were obtained from MM patients and healthy donors after informed consent was obtained in accordance with the Declaration of Helsinki protocol and approved by the institutional review board of The Tenth People's Hospital of Shanghai, Tongji University.

All MM cell lines, primary $CD138^+$ MM cells and PBMCs were cultured in RPMI-1640 medium (Gibco, Carlsbad, CA, USA) containing 10% fetal bovine serum (FBS; Gibco, BRL, USA) and 1% penicillin-streptomycin (PS; Gibco, Carlsbad, CA, USA) at 37 °C, 5% carbon-dioxide. Human BMSC line HS-5 was cultured in DMEM/HIGH GLUCOSE medium (Gibco, Carlsbad, CA, USA) containing 10% FBS and 1% PS at 37 °C, 5% carbon-dioxide. Culture medium was changed every other day.

2.2. Reagents

Rafoxanide was purchased from J&K Scientific Ltd (Shanghai, China). Recombination humaninterleukin (IL)-6 and recombination human insulin-like growth factor (IGF)-1 were purchased from R&D system (Minneapolis, MN, USA). IL-6 (25 ng/mL) and IGF-1 (25 ng/mL) were used to induce MM cell growth and proliferation. Pan-caspase inhibitor, Z-VAD-FMK, and vemurafenib were purchased from Selleck Chemicals (Houston, TX, USA). Bortezomib and lenalidomide were purchased from Sigma (Sigma-Aldrich, St, Louis, MO, USA).

2.3. Cell viability assay

MM cell lines were seeded into 96-well plates in 100 μL complate media at a density of 2×10^5 cells/mL and treated with rafoxanide (0, 5, 10, 20, 40, or 80 μM) or vemurafenib (0, 5, 10, 20, 40, or 80 nM) for indicated time. For detecting the effect of this drug on MM cells at the presence of BM microenvironment, H929 and ARP1 cells were cultured with rafoxanide (0, 10, or 20 μM) alone or in the presence of BMSC (HS-5), or cell cytokines (IL-6 and IGF-1) for 48 h. H929 and ARP1 cells were cultured with rafoxanide in combination with bortezomib or lenalidomide for 48 h. Cell viability was evaluated by Cell Counting Kit-8 (CCK8, Dojindo, Kumamoto, Japan) according to the manufacturer's instructions. Half maximal inhibitory concentration (IC_{50}) values and combination index (CI) were evaluated by using CalcuSyn software, Version 2.0 ($CI < 1$ indicates synergistic effect).

2.4. Cell apoptosis analysis

MM cell lines and PBMCs were cultured in 24-well plates at a density of 2×10^5 cells/mL and treated with rafoxanide (0, 10, or 20 μM) alone or in the presence of BMSC (GFP-HS-5), or Z-VAD-FMK (50 μM) for indicated time. Then cells were collected and washed in PBS, and incubated at room temperature for 15 min with an Annexin-V/propidium iodide (PI) (BD Pharmingen, Franklin Lakes, NJ, USA) double staining. BMMCs were stained with APC conjugated anti-CD138 (BioLegend, San Diego, CA, USA), Annexin-V, and 7-aminoactinomaycin D (7-AAD, KeyGen Biotech, Nanjing, China). Then the staining was performed according to the manufacturer's protocol. Finally, cell apoptosis were detected by a BD FASCCanto II flow cytometer (BD BioScience, San Jose, CA, USA).

2.5. DNA synthesis assay

H929 and ARP1 cells were seeded in 24-well plates at a density of 2×10^5 cells/mL and treated with rafoxanide (0, 10, or 20 μM) for 24 h. Then the 5-ethynyl-2′-deoxyuridine (EdU) incorporation analysis was performed according to the manufacturer's instruction by using EDU kit (RiboBio, Guangzhou, China). MM cells were exposed to 50 μM EDU for 2 h at 37 °C, collected and washed with PBS and fixed with 4% paraformaldehyde, followed by permeabilization with 0.5% Triton-100X (Sigma-Aldrich, St. Louis, MO, USA). Then cells were incubated with azide-conjugated Alexa Fluor 567 dye and Hoechst 33342 for 30 min respectively and visualized under a confocal laser scanning microscope

(LSM710; Zeiss, Germany) and Zen2011 software (Carl-Zeiss, Jena, Germany).

2.6. Cell cycle analysis

MM cells were cultured in 24-well plates at a density of 2×10^5 cells/mL and treated with rafoxanide (0 or 20 μM) for indicated time. Then cells were collected and washed in cold PBS, and fixed in 70% ethanol at −20 °C overnight. Next day, the fixed-cells were washed in PBS and incubated with 300 μL PI/RNase staining buffer (BD Pharmingen, Franklin Lakes, NJ, USA) at room temperature for 15 min and analyzed by flow cytometry.

2.7. Mitochondrial membrane potential analysis

The loss of mitochondrial membrane potential (MMP) occurring in apoptosis was detected by flow cytometry using JC-1 kit (Beyotime Insititute of Biotechnology, Haimen, China) according to the manufacturer's instructions. Briefly, MM cells were cultured in 24-well plates and treated with rafoxanide (0, 10, or 20 μM) for 48 h. Then cells were collected and washed in PBS, and incubated with JC-1 working solution at 37 °C for 20 min. Finally, cells were washed in JC-1 staining buffer and analyzed by flow cytometry.

2.8. Immunofluorescence analysis

MM cells were cultured in 24-well plates at a density of 2×10^5 cells/mL and treated with rafoxanide (0, 10, or 20 μM) for 24 h. Then cells were collected, washed in PBS, and fixed in 4% paraformaldehyde for 20 min. After washing in PBS, cells were blocked for 30 min with 5% BSA and ruptured with 0.2% Trinton-100X, and incubated γ-H2AX (1:200 dilution; Abcam, Cambridge, MA, USA) at 37 °C for 1 h in the incubator. Then cells were washed in PBS and followed by immunofluorescence detection using a donkey anti-rabbit antibody conjugated with fluorochrome Alexa FluorH 488 (1:400 dilution; Jackson ImmunoResearch Laboratory, USA) for 1 h in the incubator at 37 °C. After washing in PBS, cells were incubated with 49, 6-diamidino-2-pheny-lindole (DAPI) (Sigma-Aldrich, St. Louis, MO, USA) for 10 min and fluorescence analysis was performed using a confocal laser scanning microscope and Zen2011 software.

2.9. Western blot analysis

MM cells were collected, washed with cold PBS, and lysed with lysis buffer (100 mM Tris-HCl, pH 6.8, 4% SDS, 20% glycerol) on ice for 30 min. Protein concentrations were detected using the BCA method (Beyotime Insititute of Biotechnology, Haimen, China). Proteins were electrophoresed using sodium dodecyl sulfate/polyacrylamide gel electrophoresis (SDS-PAGE Bio-Rad, CA, USA) and transferred electrophoretically to membranes. The membranes blocked with 5% non-fat milk at room temperature for 1 h and were incubated with primary antibodies overnight at 4 °C. The next day, membranes were washed and incubated with the appropriate Fluorescence-conjugated secondary antibodies at room temperature for 1 h. Finally, membranes were washed and developed using the Odyssey two-color infrared laser imaging system (LICOR, Lincoln, NE, USA). Primary antibodies were as follow: anti-cleaved-caspase 3, anti-cleaved-caspase 8, anti-caspase 9, anti-Bcl-2, anti-Bcl-xl, anti-Bax, and anti-B-Raf were purchased from Cell Signaling Technology (CST, Beverly, USA); anti-CDK4, anti-CDK6, anti-cyclinD1, anti-cdc25A, anti-phospho-CHK2 (Thr68), anti-phospho-H2AX (γ-H2AX), p38 MAPK, anti-phospho-p38 MAPK, anti-phospho-Stat1, anti-phospho-ERK1/2, and anti-phospho-JNK were purchased from Abcam (Cambridge, MA, USA); anti-β-actin was purchased from Sigma (Sigma-Aldrich, St. Louis, MO, USA).

2.10. In vivo animal experiments

Male BALB/C nude mice (5 weeks old) were purchased from Shanghai Laboratory Animal Center (Shanghai, China). Mice were maintained under a 12 h light–dark cycle at 22 °C, provided water ad libitum, fed standard laboratory chow, and allowed to acclimatize for a minimum of one week. 2.5×10^6 H929 cells in 100 μL serum-free culture medium were inoculated subcutaneously into the right flank of each nude mice. When the tumors were measurable, mice were randomly divided into control and treatment groups: the vehicle-treated group (DMSO and saline) and 15 mg/kg rafoxanide-treated group (dissolved in DMSO and saline solution). Mice were administrated of DMSO, saline, and with or without rafoxanide by intraperitoneal injection every two days for a total of 14 days. Tumor size and body weight were measured every other day. Tumor volume = 0.5 ($a \times b^2$) where a is the long diameter and b is the short diameter. At the end of the treatment, mice were sacrificed. Tumors were fixed with 4% paraformaldehyde for 24 h. Then hematoxylin and eosin (HE), Ki67, cleaved-caspase 3, TUNEL, γ-H2AX, and p-p38 MAPK staining were performed. All animal-related procedures *in vivo* were approved by the Animal Care and Use Committee of The Tenth People's Hospital of Shanghai, Tongji University. This study was also approved by the Science and Technology Commission of Shanghai Municipality (ID: SYXK 2007–0006) under the permit number 2011-0111.

2.11. Histological examination staining

The tumors were fixed in 4% paraformaldehyde for 24 h, dehydrated via a graduated ethanol series, and embedded in paraffin blocks. All sections (5 μm) were dewaxed in xylene, hydrated through an upgraded ethanol series, and stained with HE. Morphological changes were examined under a light microscope at a magnification of × 200 by three pathologists who were unaware of the original specimens (CTR 6000; Leica, Wetzlar, Germany).

2.12. Immunohistochemistry

Tumor sections (5 μm) were dewaxed in xylene, hydrated through an upgraded ethanol series. For antigen retrieval, slides were boiled in EDTA (1 mM, pH 8.0) for 15 min in a microwave oven. Endogenous peroxidase activity was quenched with 0.3% hydrogen peroxide solution for 10 min at room temperature. After rinsing with PBS, slides were blocked with 5% BSA for 30 min. Slides were subsequently incubated with a polyclonal antibody against Ki-67 (1:200 dilution), cleaved-caspase 3 (1:200 dilution), γ-H2AX (1:200 dilution), and p-p38 MAPK (1:200 dilution) overnight at 4 °C respectively. Antibody binding was detected with an Envision Detection Kit, Peroxidase/DAB, Rabbit/Mouse (Gene Tech, Shanghai, China). Sections were counterstained with hematoxylin. Positive areas stained with Ki-67, and cleaved-caspase 3 were observed in all specimens under a microscope at a magnification of × 400 by three pathologists who were unaware of specimen origins.

2.13. Terminal deoxynucleotidyl transferase dUTP nick end-labeling (TUNEL) assay

Tumor sections (5 μm) were dewaxed in xylene, hydrated through an upgraded ethanol series, and detected the cell apoptosis via using TUNEL kit (Roche, Basel, Switzerland) according to the manufacturer's protocols. Cell apoptosis was evaluated by use a light microscope at a magnification of × 400 by three pathologists who were unaware of the original specimens.

2.14. Lentivirus transduction

MM cells (2×10^5 cells) were prepared and infected at a

multiplicity of infection (MOI) of 50 with control, or B-Raf V600E overexpression lentiviruses (GeneChem, Shanghai, China) according to the manufacturer's instructions, and western blot was used to validate the efficiency of B-Raf V600E overexpression.

2.15. siRNA transfection

Three small interfering RNAs (siRNAs) targeting human B-Raf were designed and constructed by RiboBio (Guangzhou, China). The siRNA sequences (5′–3′) were as follows: GGAGCATAATCCACCATCA, GGAG AATGTTCCACTTACA, and CAAGCTAGATGCACTCCAA. The negative control siRNA and B-Raf siRNAs were transfected into B-Raf V600E-OE MM cells using Lipofectamine 3000 transfection reagent (Invitrogen, Carlsbad, CA, USA). The first siRNA sequence was used to construct the knockdown of B-Raf V600E, and western blot was used to validate the efficiency of B-Raf V600E knockdown.

2.16. Statistical analysis

The data were expressed as mean ± standard deviation (SD). Student's t-test was performed as appropriate using SPSS v20.0 software (IBM, Armonk, NY, USA). Significance was established at a p value of less than 0.05.

3. Results

3.1. Rafoxanide exerts anti-proliferative activity in MM cell lines and overcomes the protective effect of the BM microenvironment on MM cells in vitro

We investigated the effect of rafoxanide in MM cell lines (H929, H929R, ARP1, OCI-MY5, MM1S, RPMI8226, OPM2, and U266) using the CCK8 assay. Our data showed that the viability of MM cells was significantly inhibited after treatment with rafoxanide for 48 h (Fig. 1A). The half-maximal inhibitory concentration (IC_{50}) of rafoxanide at doses of 5, 10, 20, 40, and 80 μM was determined in each of these MM cell lines using CalcuSyn software, Version 2.0, and the results were 19.2 μM (H929), 40.1 μM (H929R), 19.3 μM (ARP1), 27.8 μM (OCI-MY5), 47.2 μM (MM1S), 27.3 μM (RPMI8226), 22.4 μM (OPM2), and 21.6 μM (U266). Interestingly, we found that rafoxanide induces a dose- and time-dependent cytotoxicity in H929, ARP1, and OCI-MY5 cells (Fig. 1B–D). Additionally, rafoxanide could induce significant cytotoxicity in lymphoma cells and other human cancer cells via detecting the cell viability using the CCK8 assay (Supplementary Fig. S1). These findings suggested that rafoxanide has potent anticancer activity.

MM is a BM microenvironment-dependent malignancy, and BMSC, IL-6 and IGF-1 promote MM growth, migration, and survival [17,18]. We investigated whether rafoxanide could protect against the effect of the BM microenvironment on MM cells. H929 and ARP1 cells were cultured with rafoxanide (0, 10, or 20 μM) alone or in the presence of BMSC, IL-6 and IGF-1 for 48 h. Our results showed that BMSC and cytokines (IL-6 and IGF-1) promoted the growth of MM cells, while rafoxanide treatment could induce cell cytotoxicity in the presence of BMSC (Fig. 1E), as well as IL-6 and IGF-1 (Fig. 1F and G). As shown in Fig. 1H and I, rafoxanide treatment also could induce MM cells apoptosis even in the presence of BMSC. Moreover, rafoxanide treatment does not affect the viability of BMSC and has no apparent apoptosis in BMSC (Fig. 1E, H and I). These data suggested that rafoxanide not only directly targets MM cells, but also overcomes the protective effect of the MM-host BM microenvironment.

3.2. Rafoxanide induces obvious apoptosis in MM cells and has no significant effect on normal PBMCs in vitro

We next evaluated the effect of rafoxanide on apoptosis in MM cells via Annexin-V/PI double staining using flow cytometry. After treatment with rafoxanide (0, 10, or 20 μM) for 24, 48, or 72 h, analysis of apoptosis showed that rafoxanide induces marked apoptosis in H929, ARP1, and OCI-MY5 cells in a dose-dependent manner (Fig. 2A–D). Western blot analysis further confirmed that rafoxanide induced apoptosis by increasing the expression of cleaved-caspase 3, cleaved-caspase 8, and cleaved-caspase 9, as well as reducing Bcl-2 and Bcl-xl and up-regulating Bax (Fig. 2E). Meanwhile, we analyzed the MMP, an indicator of cell apoptosis, in MM cells by flow cytometry using a JC-1 MMP kit. As shown in Fig. 3A and B, MMP was significantly reduced in H929, ARP1, and OCI-MY5 cells after treatment with rafoxanide for 48 h. Moreover, to further determine the dependence of rafoxanide-induced apoptosis on the caspase pathway, we next analyzed the effect of a pan-caspase inhibitor named Z-VAD-FMK. Importantly, using flow cytometry with Annexin-V/PI double staining, our results indicated that Z-VAD-FMK significantly blocked rafoxanide-induced apoptosis of H929, ARP1 and OCI-MY5 cells (Fig. 3C and D). These findings suggested that rafoxanide triggers both extrinsic and intrinsic apoptotic pathways, and that rafoxanide-induced apoptosis in MM is dependent on the caspase pathway.

To further confirm the anti-MM activity of rafoxanide, we evaluated the effect of rafoxanide on $CD138^+$ MM cells isolated from the BM of MM patients (Table 1) by flow cytometric analysis. As shown in Fig. 3E and F, rafoxanide induced significant apoptosis in $CD138^+$ MM cells, while no apparent apoptosis was observed in normal PBMCs (Fig. 3G and H), indicating that rafoxanide has no toxicity in normal PBMCs and is a favorable drug for the treatment of MM.

3.3. Rafoxanide inhibits DNA synthesis and induces cell cycle arrest in MM cells in vitro

As rafoxanide was able to inhibit MM cell viability, we next evaluated whether this drug could affect DNA synthesis in MM cells using EdU incorporation assay. Our results showed that rafoxanide greatly reduced the level of EDU in H929 and ARP1 cells (Fig. 4A and B), suggesting that the DNA synthesis of MM cells was markedly inhibited after treatment with rafoxanide for 24 h. Additionally, we analyzed the effect of rafoxanide on the MM cell cycle using flow cytometric analysis. As shown in Fig. 4C and D, rafoxanide treatment caused H929, ARP1, and OCI-MY5 cells to accumulate in G_0G_1 phase. Meanwhile, western blot analysis further confirmed rafoxanide-induced MM cell cycle arrest in G_0G_1 phase by reduction of the protein expression of cyclinD1, CDK4, CDK6, decreased cdc25A, and increased phosphorylation of CHK2, further suggesting that rafoxanide-induced cell cycle arrest is mediated by the cdc25A-degradation pathway (Fig. 4E).

3.4. Rafoxanide enhances the DNA damage response and suppresses the p38 MAPK pathway in MM cells in vitro

To determine whether rafoxanide affects DNA damage, we next analyzed the expression of γ-H2AX (a marker of DNA damage) after treatment of MM cells with rafoxanide for 24 h. The results of immunofluorescence analysis showed that the presence of γ-H2AX nuclear foci was markedly increased in H929 and ARP1 cells after administration of rafoxanide (Fig. 5A). Meanwhile, we evaluated the protein level of γ-H2AX in H929 and ARP1 cells. Importantly, consistent with the results of immunofluorescence analysis, the protein expression of γ-H2AX in H929 and ARP1 cells was increased after rafoxanide treatment (Fig. 5B), further indicating that rafoxanide can enhance the DNA damage response in MM cells. Besides DNA damage, the MAPK pathway also plays an important role in MM. Thus, we analyzed changes in the MAPK pathway after treatment with rafoxanide. Interestingly, we found that rafoxanide was able to significantly suppress the p38 MAPK pathway by reducing the phosphorylation of p38 MAPK, whereas the expression of phosphorylated ERK1/2 and phosphorylated JNK remained unchanged. The down-regulation of Stat1 phosphorylation, a downstream protein of p38 MAPK, further confirmed the inhibition of

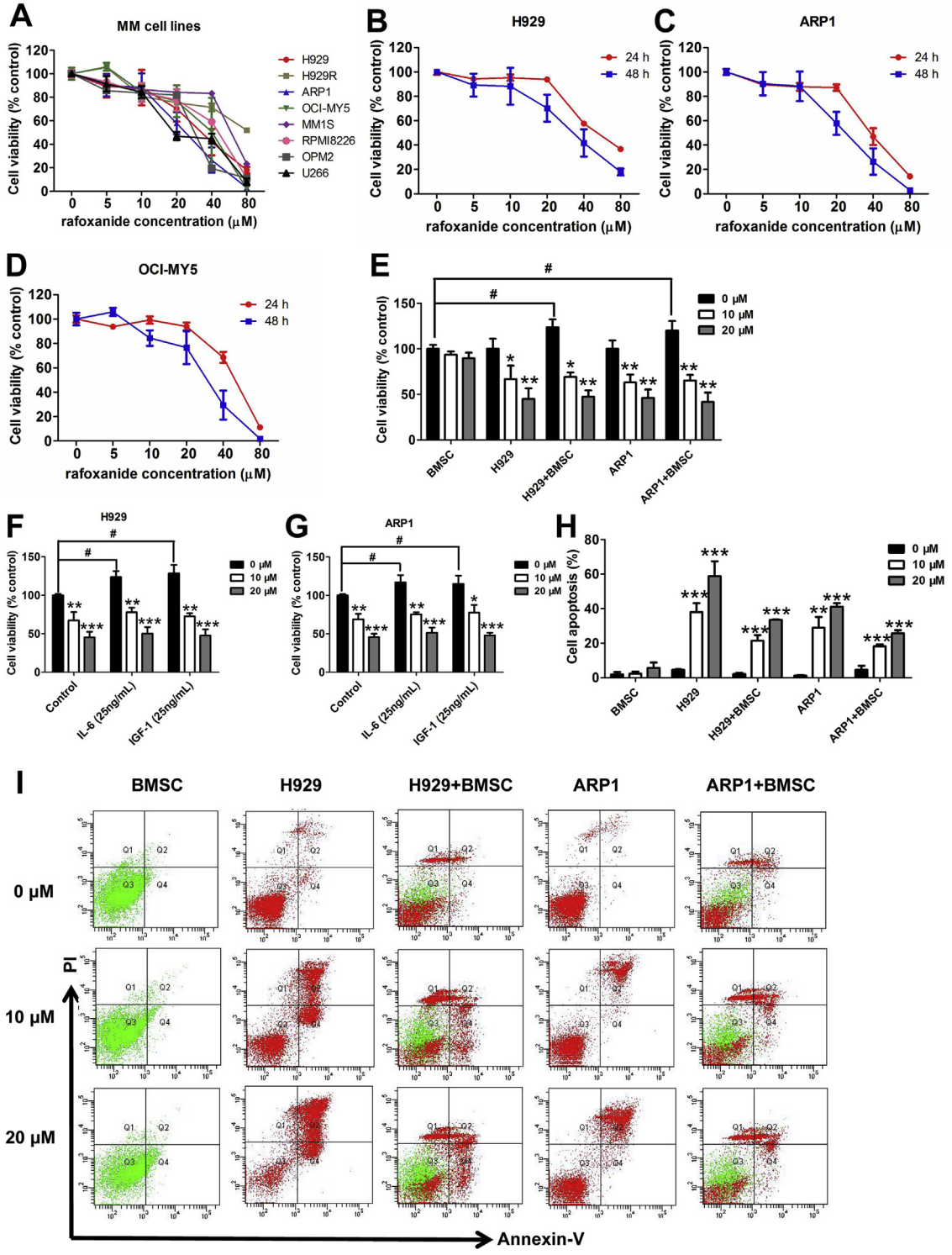

Fig. 1. Rafoxanide exerts cytotoxic effects on MM cells and overcomes the protective effect of the BM microenvironment. (A) MM cell lines were treated with rafoxanide (0, 5, 10, 20, 40, or 80 μM) for 48 h and cell viability was analyzed using a CCK8 kit. (B–D) H929, ARP1, and OCI-MY5 cells were treated with rafoxanide (0, 5, 10, 20, 40, or 80 μM) for 24 or 48 h, and cell viability was measured using a CCK8 kit. (E) BMSC, H929, both H929 and BMSC, ARP1, or both ARP1 and BMSC cells were treated with rafoxanide (0, 10, or 20 μM) for 48 h, and cell viability was analyzed by CCK8 kit. Data are represented as mean ± SD of three independent experiments and $*p \le 0.05$, $**p \le 0.01$, by unpaired two-tailed Student's t tests, compared with the 0 μM group; $^{\#}p \le 0.05$, by unpaired two-tailed Student's t tests. (F and G) H929 and ARP1 cells were treated with rafoxanide (0, 10, or 20 μM) and cultured in the presence of IL-6 or IGF-1 for 48 h, and cell viability was detected using a CCK8 kit. Data are represented as mean ± SD of three independent experiments and $*p \le 0.05$, $**p \le 0.01$, $***p \le 0.001$, by unpaired two-tailed Student's t tests, compared with the 0 μM group; $^{\#}p \le 0.05$, by unpaired two-tailed Student's t tests. (H) The percentage of Annexin-V positive cells. Data are represented as mean ± SD of three independent experiments and $**p \le 0.01$, $***p \le 0.001$, by unpaired two-tailed Student's t tests, compared with the 0 μM group. (I) BMSC, H929, both H929 and BMSC, ARP1, or both ARP1 and BMSC cells were treated with rafoxanide (0, 10, or 20 μM) for 48 h, and apoptosis was detected by Annexin-V/PI staining followed by flow cytometry. Green represents BMSC HS-5 cells, and red represents MM cells.

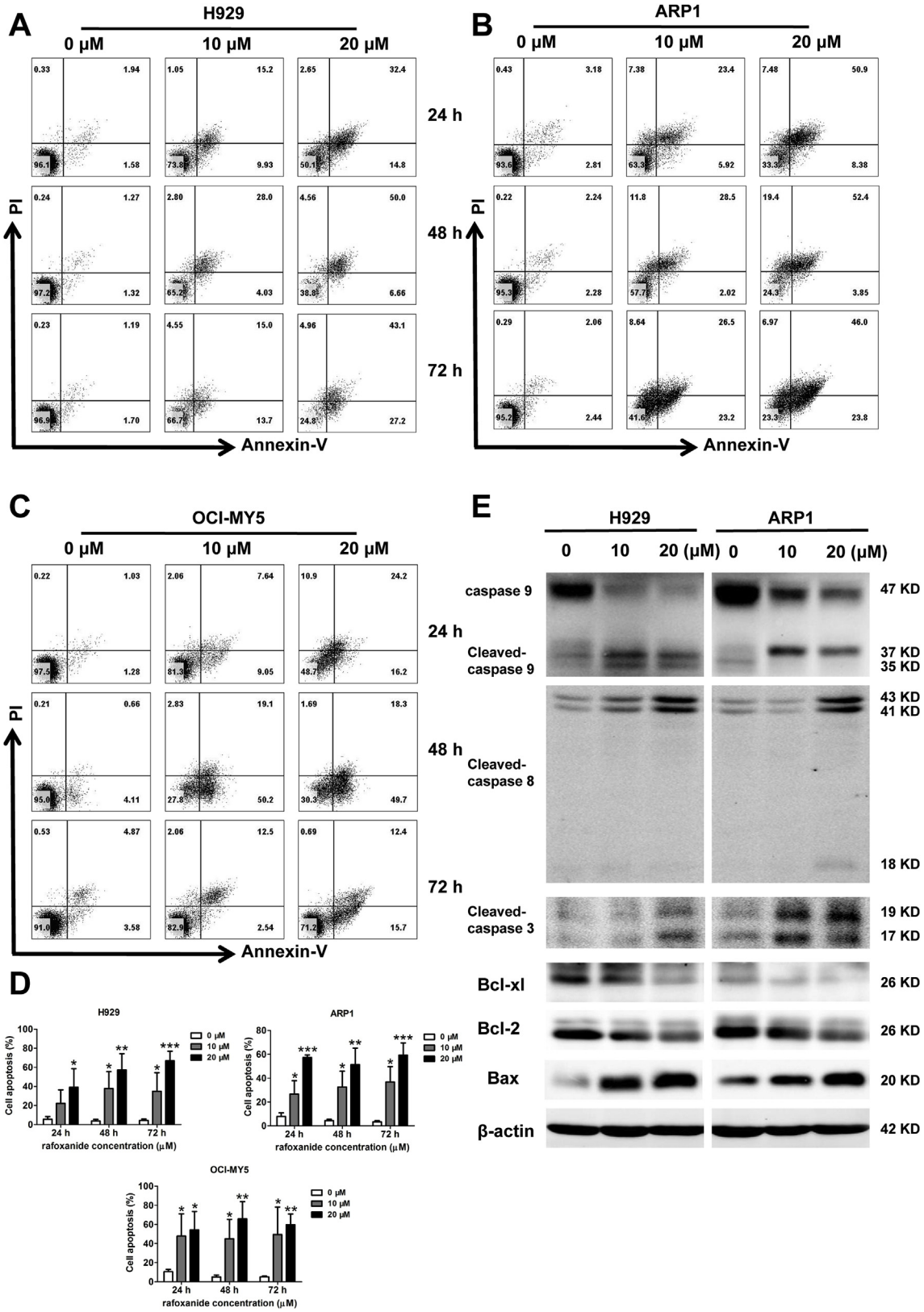

Fig. 2. Rafoxanide induces apoptosis in MM cells *in vitro*. (A–C) H929, ARP1, and OCI-MY5 cells were treated with rafoxanide (0, 10, or 20 μM) for 24, 48, or 72 h, and apoptosis was detected by Annexin-V/PI staining followed by flow cytometry. (D) The percentage of Annexin-V positive cells. Data are represented as mean ± SD of three independent experiments and $*p \leq 0.05$, $**p \leq 0.01$, $***p \leq 0.001$, using unpaired two-tailed Student's t tests, compared with the 0 μM group. (E)Western blot analysis of cleaved-caspase 3, cleaved-caspase 8, cleaved-caspase 9, Bcl-xl, Bcl-2 and Bax in H929 and ARP1 cells after treatment with rafoxanide (0, 10, or 20 μM) for 48 h.

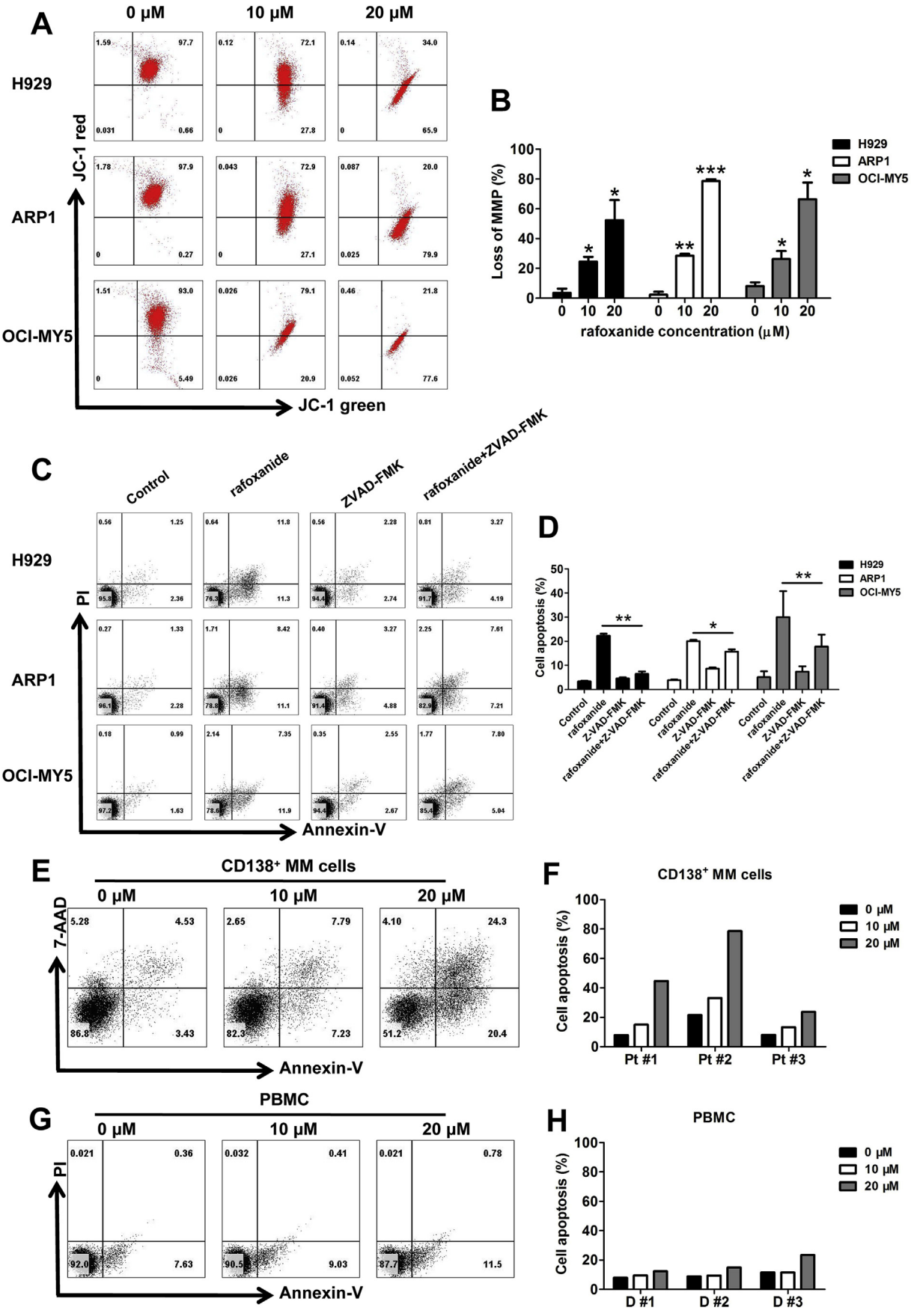

(caption on next page)

Fig. 3. Rafoxanide-induced apoptosis in MM cell lines and patient MM cells, while no apparent apoptotic effect on normal cells. (A) H929, ARP1, and OCI-MY5 cells were treated with rafoxanide (0, 10, or 20 μM) for 48 h, and the level of MMP was analyzed using a JC-1 MMP kit using flow cytometry. (B)The percentage of JC-1 MMP green-positive cells. Data are represented as mean ± SD of three independent experiments and $*p \leq 0.05$, $**p \leq 0.01$, $***p \leq 0.001$, by unpaired two-tailed Student's t tests, compared with the 0 μM group. (C) H929, ARP1 and OCI-MY5 cells were pretreated with pan-caspase (Z-VAD-FMK) for 2 h, then rafoxanide (0 or 10 μM) was added for another 48 h, and apoptosis was evaluated by Annexin-V/PI double staining using flow cytometry. (D) The percentage of Annexin-V positive cells. Data are represented as mean ± SD of three independent experiments and $*p \leq 0.05$, $**p \leq 0.01$, by unpaired two-tailed Student's t tests, compared with the rafoxanide-treated group. (E and F) Primary $CD138^+$ MM cells from patients were treated with rafoxanide (0, 10, or 20 μM) for 48 h, and apoptosis was detected by anti-CD138/Annexin-V/7-AAD staining using flow cytometry. Pt represents patient. (G and H) PBMCs were treated with rafoxanide (0, 10, or 20 μM) for 48 h, and apoptosis was detected by Annexin-V/PI double staining using flow cytometry. D represents healthy donor.

the p38 MAPK pathway after rafoxanide treatment (Fig. 5C).

3.5. Rafoxanide inhibits tumor growth in an MM xenograft model in vivo

We established a human myeloma xenograft model to further investigate the anti-MM activity of rafoxanide *in vivo*. Five-week-old nude mice were injected subcutaneously with 2.5×10^6 H929 cells. Mice were treated with or without rafoxanide (15 mg/kg body weight every two days) by intraperitoneal injection for a total of 14 days. Tumor growth and tumor weight in rafoxanide-treated groups was inhibited compared with the vehicle-treated group (Fig. 6A–C). Meanwhile, we evaluated the body weight of vehicle-treated and rafoxanide-treated mice. Results showed no significant body weight changes in these two groups, indicating that rafoxanide was well tolerated (Fig. 6D). In addition, HE staining showed an obvious increase of cell shrinkage and fragmentation in harvested tumors from the rafoxanide-treated group compared with the vehicle-treated group (Fig. 6E). Meanwhile, we found no obvious histological changes in the heart, liver, lung, or kidney in any of the mice (Supplementary Fig. S2), further suggesting that the side-effects of rafoxanide were minimal. In addition, rafoxanide treatment markedly inhibited tumor proliferation, indicated by reduced Ki-67 staining, and induced tumor apoptosis, indicated by increased numbers of cleaved-caspase 3- and TUNEL-positive cells (Fig. 6F). Meanwhile, we examined the expression of γ-H2AX and p-p38 MAPK in harvest tumors, results showed that rafoxanide enhances DNA damage response by increasing the expression of γ-H2AX and inhibits the activation of p38 MAPK pathway via suppressing the expression of p-p38 MAPK (Fig. 6F), consistent with our *in vitro* results. These findings suggested that rafoxanide has potent anti-MM activity *in vivo*.

3.6. Rafoxanide synergizes with bortezomib or lenalidomide in MM cells in vitro

To examine whether rafoxanide could be used in combination therapy, we detected MM cells viability of rafoxanide in combination with bortezomib or lenalidomide. As shown in Fig. 7A–D, combination of rafoxanide and bortezomib or lenalidomide significantly induced synergistic cytotoxicity in H929 and ARP1 cells, with the combination index (CI) < 1.

3.7. Different effect of rafoxanide in wild type B-Raf, B-Raf V600E overexpressed, and B-Raf V600E knocked down MM cells

Our previous study has indicated rafoxanide is a potent B-Raf V600E inhibitor with IC_{50} value of 0.07 μM, which is appreciable compared to the positive control vemurafenib (a marketed drug targeting B-Raf V600E; IC_{50}: 0.17 μM). Moreover, vemurafenib inhibited mutated and wild type B-Raf with the same IC_{50} level, while rafoxanide showed high potency against the wild type B-Raf and B-Raf V600E [12], suggesting that rafoxanide could inhibit both wide type B-Raf and B-Raf V600E. To determine whether rafoxanide is a B-Raf V600E inhibitor, we firstly examined the expression of B-Raf in MM cell lines by using western blot analysis (Supplementary Fig. S3), then constructed B-Raf V600E overexpressed H929 and ARP1 cells by lentivirus transduction (Fig. 8A), and B-Raf V600E knocked down H929 and ARP1 cells by siRNA transduction (Fig. 8B). Our CCK8 and flow cytometry analysis showed that rafoxanide suppresses the growth of H929 and ARP1 cells while overexpression of B-Raf V600E could rescue cells from rafoxanide-induced proliferative inhibition and apoptosis. Additionally, knockdown of B-Raf V600E could induce cytotoxicity and apoptosis towards rafoxanide compared with B-Raf V600E-OE H929 and ARP1 cells, while no significant difference compared with the wild type group (Fig. 8C–F). However, CCK8 analysis showed the IC_{50} of rafoxanide in these MM cells is 20–40 μM, while 10–20 nM for vemurafenib, and vemurafenib has the similar IC_{50} level in these cells (Fig. 8C and D). These data suggested that rafoxanide has anti-proliferation effect on both wild type and B-Raf V600E mutated MM cells. And the weaker anti-MM activity of rafoxanide than vemurafenib *in vitro* may indicate other potential mechanisms besides targeting B-Raf V600E mutation.

4. Discussion

Rafoxanide, an anthelmintic drug of the salicylanilide class, is used for the treatment of both mature and immature stages of liver fluke in cattle and sheep [19]. An important finding indicated that rafoxanide exhibits desirable properties for repositioning as a human agent [11]. We previously demonstrated that rafoxanide is a potent B-Raf V600E inhibitor via molecular docking with halogen bonding scoring function and bioassay [12]. The B-Raf mutation causes constitutive activation of the MAPK pathway and both of B-Raf and MAPK play significant roles in MM cell proliferation and growth [13]. Despite advances in treatment options over recent decades, MM is still an incurable hematological malignancy with accumulation of plasma cells in the BM [20]. Therefore, we investigated the effects of rafoxanide on MM cells. Our present study is the first to demonstrate that this anthelmintic drug has antitumor activity and exerts effective cytotoxicity on MM cells both *in vitro* and *in vivo* (Fig. 7E).

In our *in vitro* study, we found that rafoxanide markedly reduces the

Table 1
The characteristics of MM patients.

Gender	Age (years)	newly diagnosed or relapsed/refractory	prior treatments	FISH
Female	55	newly diagnosed	—	t(4; 14) translocation p53(17p13.1) deletion
Male	72	newly diagnosed	—	t(11; 14) translocation CKS1B(1q21) abnormality
Female	51	relapsed/refractory	VAD	RB1(13q14) deletion CKS1B(1q21) abnormality

Abbreviation: FISH, Fluorescent in situ hybridization; VAD, Dexamethasone + Doxorubicin + Vincristine.

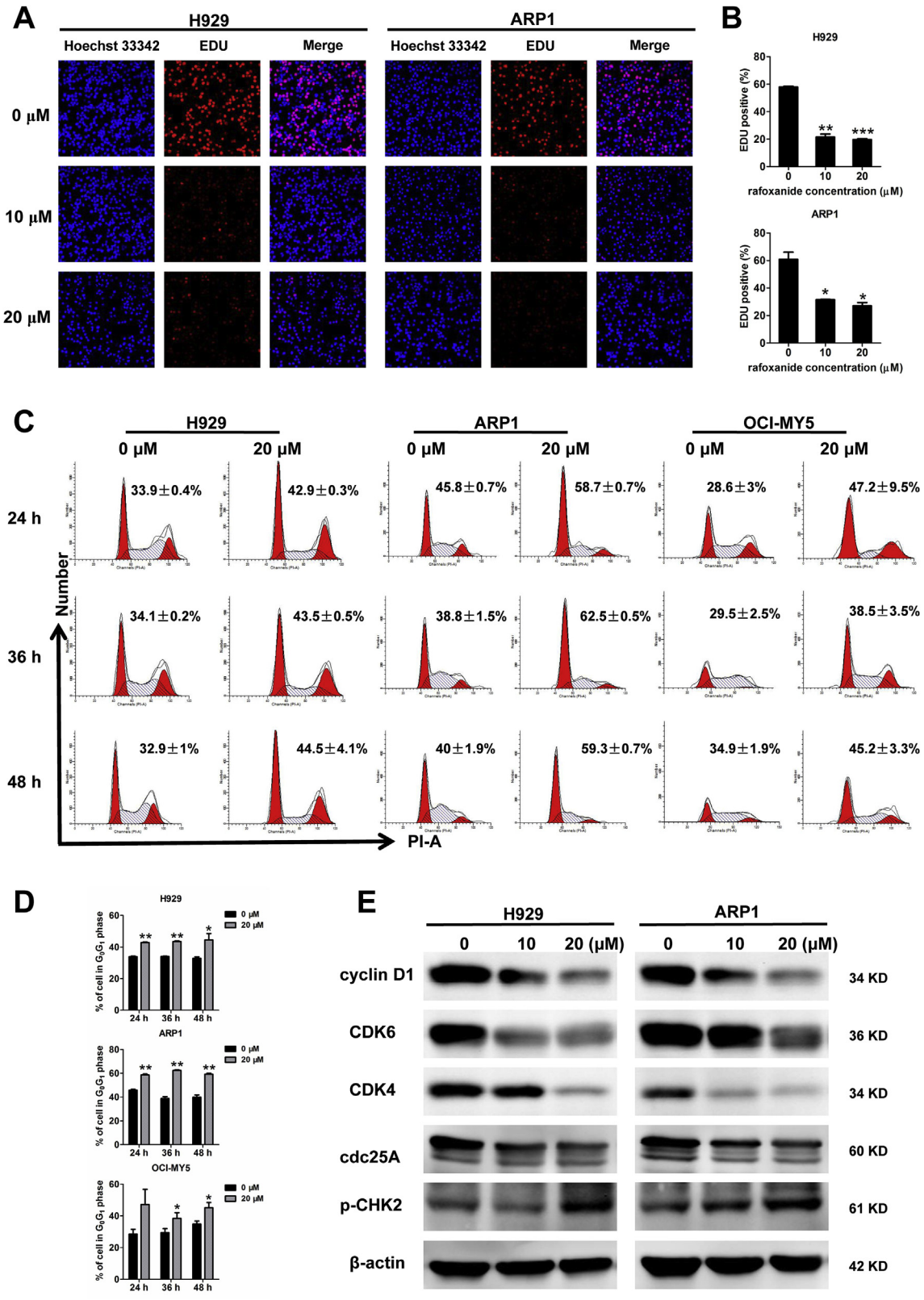

Fig. 4. Rafoxanide inhibits DNA synthesis and causes G_0G_1 cell cycle arrest in MM cells *in vitro*. (A) H929 and ARP1 cells were treated with rafoxanide (0, 10, or 20 μM) for 24 h, and DNA synthesis was measured using an EDU incorporation kit. EDU incorporation was observed using laser scanning confocal microscopy. Red indicates EDU-positive cells, at 250 × magnification. (B) The percentage of EDU-positive cells. Data are represented as mean ± SD of three independent experiments and $*p \leq 0.05$, $**p \leq 0.01$, $***p \leq 0.001$, by unpaired two-tailed Student's t tests, compared with the 0 μM group. (C) H929, ARP1, and OCI-MY5 cells were treated with rafoxanide (0 or 20 μM) for 24, 36, or 48 h, and the cell cycle was analyzed by PI staining using flow cytometry. (D) The percentage of the cell population in G_0G_1 phase. Data are represented as mean ± SD of three independent experiments and $*p \leq 0.05$, $**p \leq 0.01$, by unpaired two-tailed Student's t tests, compared with the 0 μM group. (E) Western blot analysis of cyclinD1, CDK4, CDK6, cdc25A, and p-CHK2 in H929 and ARP1 cells after treatment with rafoxanide (0, 10, or 20 μM) for 24 h.

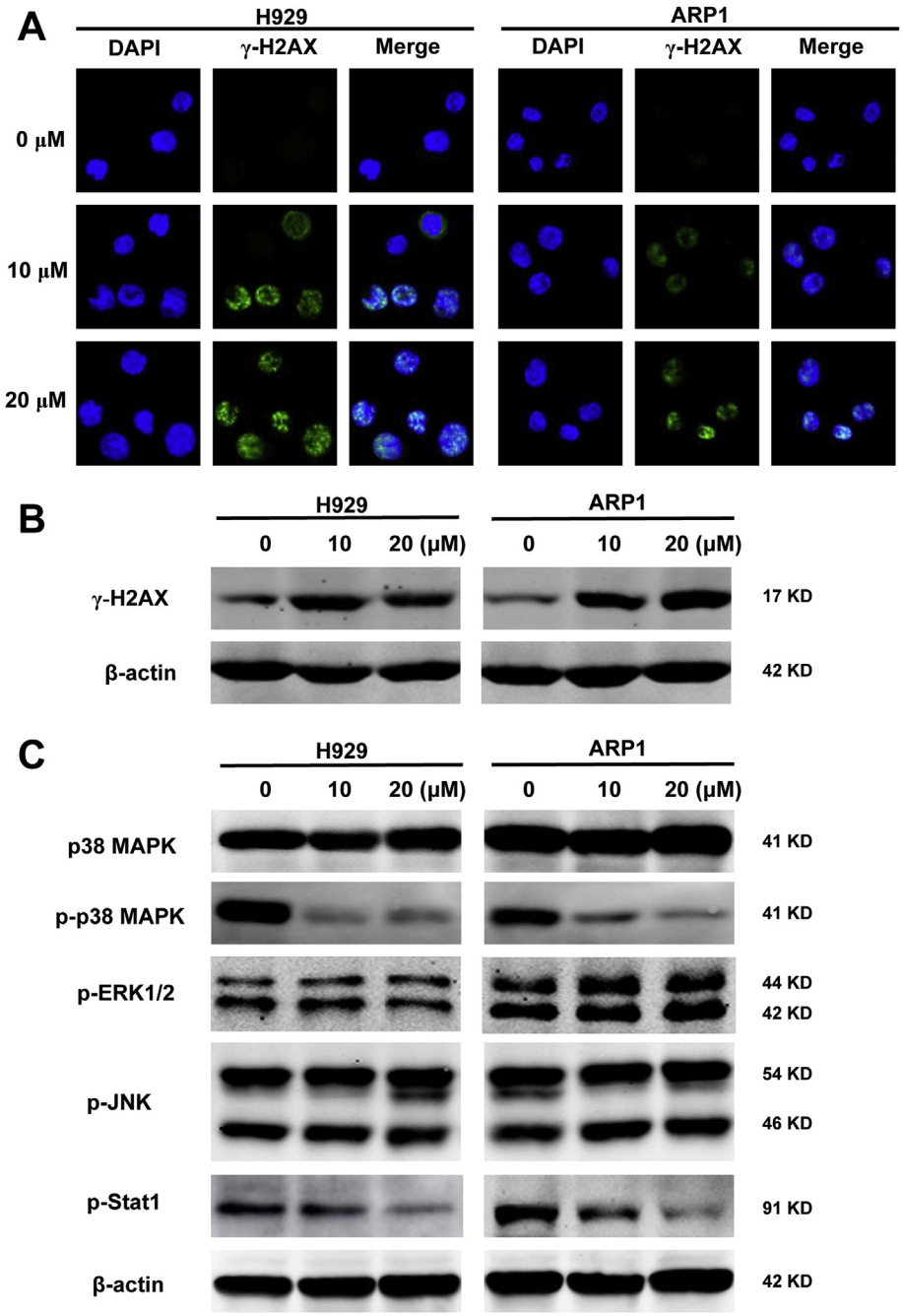

Fig. 5. Rafoxanide enhances the DNA damage response and suppresses the p38 MAPK pathway in MM cells *in vitro*. (A) Immunofluorescence staining of γ-H2AX in H929 and ARP1 cells after treatment with rafoxanide (0, 10, or 20 μM) for 24 h. The presence of γ-H2AX foci was observed using laser scanning confocal microscopy. Green indicates γ-H2AX-positive cells; 630 × magnification. (B) Western blot analysis of γ-H2AX in H929 and ARP1 cells after treatment with rafoxanide (0, 10, or 20 μM) for 24 h. (C) Western blot analysis of p38 MAPK, p-p38 MAPK, p-Stat1, p-ERK1/2, and p-JNK in H929 and ARP1 cells after treatment with rafoxanide (0, 10, or 20 μM) for 48 h.

viability of a series of MM cell lines and has a dose- and time-dependent effect in H929, ARP1 and OCI-MY5 cells, further suggesting that rafoxanide has anti-proliferative activity in MM cells. There is a growing body of evidence indicating that MM is highly dependent on the BM microenvironment [21,22], so there is an urgent need to develop novel anti-MM drugs to overcome the protective effect of the BM microenvironment. Our present data show that rafoxanide significantly inhibits the growth of MM cells even in the presence of BMSC and cytokines IL-6 and IGF-1. Importantly, rafoxanide treatment also induces the apoptosis of MM cells in the presence of BMSC, while has no significant effect in BMSC. These findings suggest that rafoxanide not only directly targets MM cells, but also confers the ability to overcome the protective effect of the BM microenvironment on MM cells.

Several studies have indicated that anti-proliferative activity of drugs is associated with apoptosis and cell cycle arrest [23,24]. Apoptosis, a main mechanism in cell death, could be triggered by intrinsically or extrinsically via death signal pathways, including caspases, inhibitors of apoptosis proteins, B cell lymphoma (Bcl)-2 family, tumor necrosis factor (TNF) receptor gene family, or p53 gene [25]. Therefore, we first evaluated apoptosis of MM cells after treatment with rafoxanide. Consistent with the results from CCK8 assay, rafoxanide induced cell apoptosis in both MM cell lines and primary $CD138^+$ MM cells, whereas no apparent apoptosis was observed in healthy PBMCs. Moreover, we further confirmed rafoxanide-induced cell apoptosis by activation of caspases, including up-regulation of the expression of cleaved-caspase 3, cleaved-caspase 8, and cleaved-caspase 9, as well as down-regulation of the protein levels of Bcl-2 and Bcl-xl along with increasing levels of Bax in MM cells. MMP, an indicator of mitochondrial membrane permeability, is decreased during early apoptosis [26]. Interestingly, we showed that rafoxanide could regulate the loss of MMP. Moreover, we also found that a pan-caspase inhibitor (Z-VAD-FMK) impaired the effect of rafoxanide in inducing MM apoptosis.

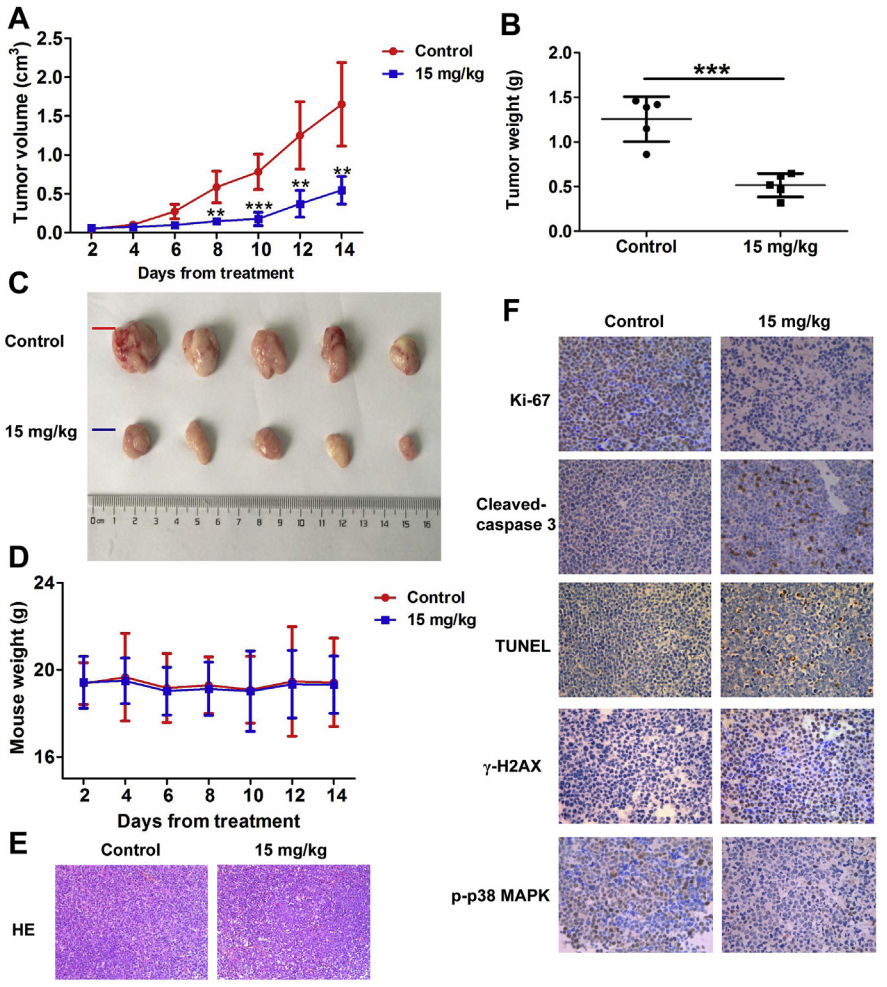

Fig. 6. Rafoxanide inhibits tumor growth in an MM xenograft model *in vivo*. (A) H929 cells were injected subcutaneously into mice and within two weeks tumors had formed. The mice were treated with vehicle or 15 mg/kg rafoxanide every two days for a total of 14 days via intraperitoneal injection after tumor formation. Tumor size was measured every other day. Data are represented as mean ± SD and $^{**}p \leq 0.01$, $^{***}p \leq 0.001$, by unpaired two-tailed Student's t tests, compared with the control group; n = 5 mice/group. (B) Tumor weight was evaluated at 14 days. Data are represented as mean ± SD and $^{***}p \leq 0.001$ by unpaired two-tailed Student's t tests, compared with the control group, 5 mice/group. (C) Gross appearance of tumors. (D) The body weight of each mouse was measured every other day. Data are represented as mean ± SD, and analyzed by unpaired two-tailed Student's t tests. (E) HE staining of tumor sections for tumor histology after rafoxanide treatment; 200 × magnification. (F) Immunohistochemical staining of Ki-67, cleaved-caspase 3, TUNEL, γ-H2AX, and p-p38 MAPK for the detection of cell proliferation, cell apoptosis, DNA damage and p38 MAPK activation *in vivo* after rafoxanide treatment. Positive cells in tumor sections stained with Ki-67, cleaved-caspase 3, TUNEL, γ-H2AX, and p-p38 MAPK are shown in dark brown; 400 × magnification.

These data suggest that rafoxanide induces MM apoptosis via both extrinsic and intrinsic apoptotic pathways, and that rafoxanide-induced cell apoptosis is regulated via MMP levels and the caspase pathway.

Cell cycle arrest induced by anti-tumor inhibitor could result in cell death via apoptosis in MM [27]. We found that rafoxanide induced inhibition of DNA synthesis, as well as arrest of MM cells in G_0G_1 phase. CyclinD1/CDK4/CDK6 complex, an important complex in the G_0G_1 phase, plays a vital role in regulating the progression from G_0G_1 phase to the G_2M phase [28]. Thus, we detected the expression of this complex in MM cells after rafoxanide treatment. Importantly, our western blot results indicated that rafoxanide-induced G_0G_1 phase arrest is associated with reduced protein expression of cyclinD1, CDK4, and CDK6, further suggesting that rafoxanide could induce G_0G_1 phase arrest of MM cells. Meanwhile, the results showed that rafoxanide decreases the expression of cdc25A, while increases p-CHK2. It is known that CHK2 plays a significant role in the DNA damage response pathway, which can be activated in response to DNA damage and directly regulate cdc25A that associated with cell cycle control [29]. These findings show that rafoxanide-induced cell cycle arrest is mediated by the cdc25A-degradation pathway, and this arrest could further trigger DNA damage response. γ-H2AX also has an important role in the DNA damage response, and the presence of γ-H2AX nuclear foci is the hallmark of DNA double-strand breaks [30]. Thus, we analyzed the expression of γ-H2AX in MM cells after treatment with rafoxanide. The data showed that rafoxanide increases the presence of γ-H2AX nuclear foci in MM cells and activates the phosphorylation of H2AX, suggesting that rafoxanide enhances the DNA damage response. Several series of studies have reported that the induction of cell apoptosis is associated with DNA damage response pathway or MAPK pathway [31,32]. Furthermore, these pathways are involved in the cellular responses, such as cell proliferation, differentiation, migration and apoptosis [33,34]. Moreover, as rafoxanide is a potent B-Raf V600E inhibitor [12], the MAPK pathway could be activated via a B-Raf mutation [16], and a recent study reported that PLX8394, a new generation B-Raf inhibitor, could selectively inhibit B-Raf in colonic adenocarcinoma cells and prevent paradoxical MAPK pathway activation [35]. Therefore, we further investigated whether rafoxanide affects the activation of MAPK pathway. Interestingly, our data showed that rafoxanide could inhibit activation of the p38 MAPK pathway by reducing the phosphorylation of p38 MAPK, as well as down-regulating phosphorylation of Stat1 (a downstream of p38 MAPK). Taken together, our results suggest that enhancement of the DNA damage response and inhibition of the p38 MAPK pathway play important roles in rafoxanide-induced apoptosis in MM cells.

To further confirm the anti-MM activity of rafoxanide, we next established an MM xenograft mouse model *in vivo*. Our data showed that rafoxanide not only markedly inhibits tumor growth, but also has no apparent toxicity in mice. Meanwhile, immunohistochemical staining of harvested tumors confirmed rafoxanide-induced anti-proliferation, pro-apoptotic effects, enhancement of DNA damage response, and suppression of p38 MAPK activation in MM cells. Consistent with our *in vitro* study, these *in vivo* results further indicate that rafoxanide has potent anti-MM activity. Additionally, we found that 10–20 μM rafoxanide induced apoptosis in patient $CD138^+$ MM cells but did not affect normal PBMCs. Injection of 15 mg/kg dose of rafoxanide every two days for a total of 14 days retarded tumor growth but did not reduce body weight or cause heart/liver/lung/kidney damage in mice. Therefore, our preliminary results indicate that rafoxanide is a well-

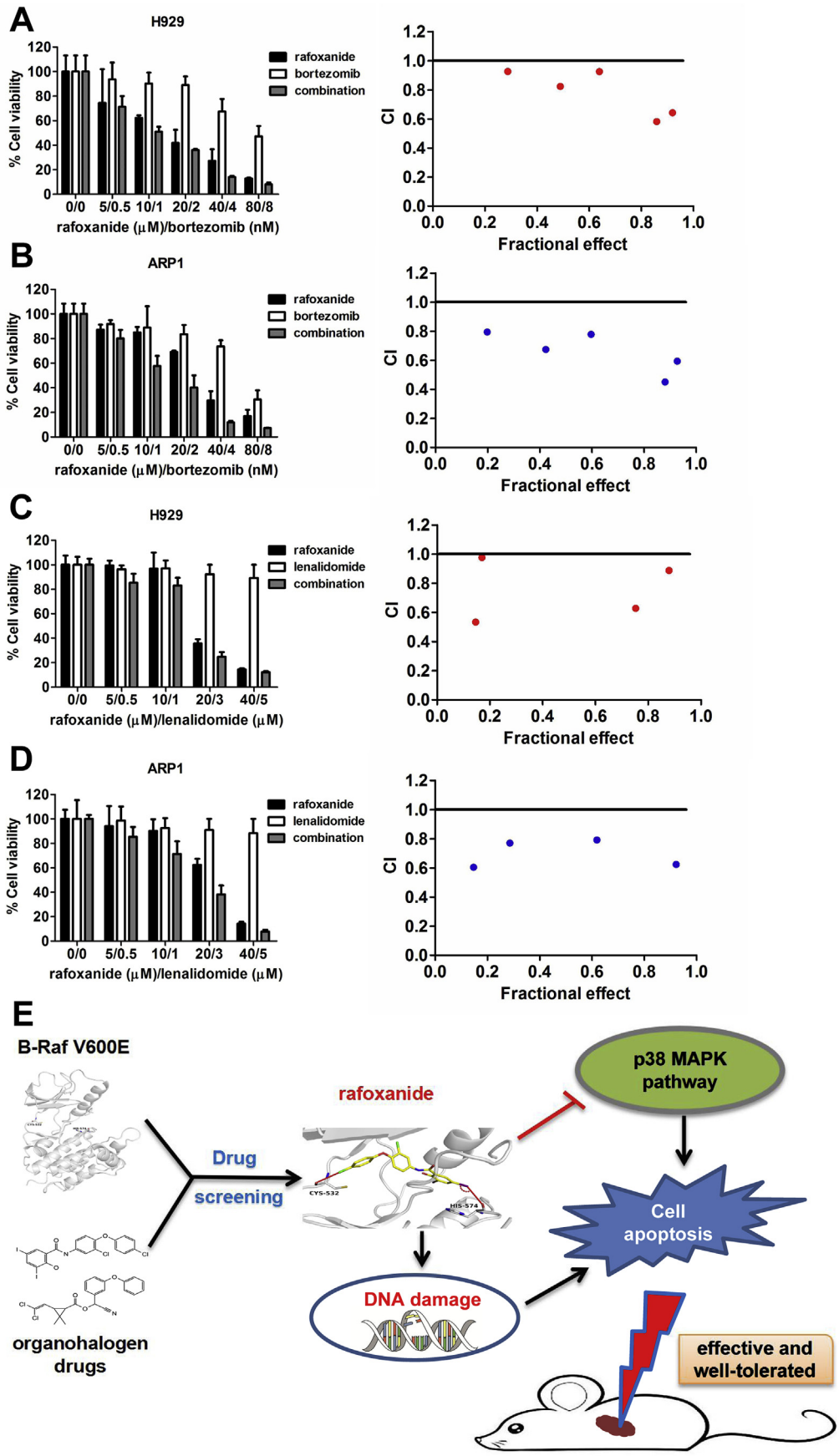

Fig. 7. Rafoxanide synergizes with bortezomib or lenalidomide in MM cells *in vitro*. (A–B) H929 and ARP1 cells were treated with rafoxanide, bortezomib or the combination of rafoxanide and bortezomib for 48 h, then cell viability was analyzed using a CCK8 kit, CI < 1 indicates synergistic activity by using CalcuSyn software, Version 2.0. (C–D) H929 and ARP1 cells were treated with rafoxanide, lenalidomide or the combination of rafoxanide and lenalidomide for 48 h, then cell viability was analyzed using a CCK8 kit, synergistic anti-MM activity was analyzed as in panel A–B. (E) The molecular mechanism of rafoxanide effect on MM.

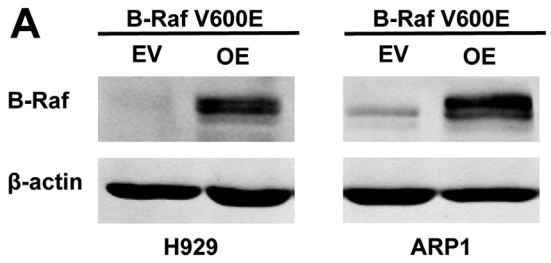

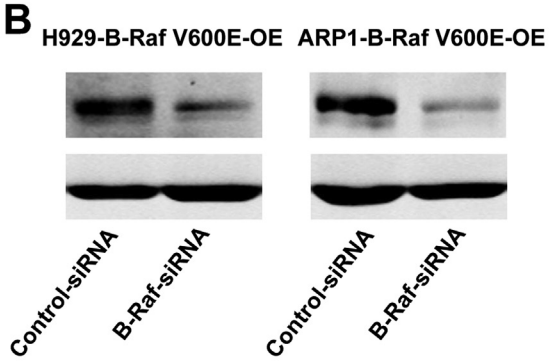

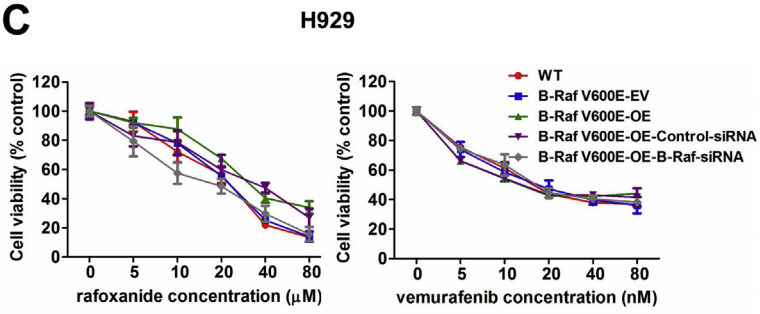

H929 Cell lines	rafoxanide IC_{50} (μM)	vemurafenib IC_{50} (nM)
WT	21.67	22.01
B-Raf V600E-EV	22.93	22.12
B-Raf V600E-OE	38.74	19.80
B-Raf V600E-OE-Control-siRNA	31.78	19.36
B-Raf V600E-OE-B-Raf-siRNA	19.12	24.09

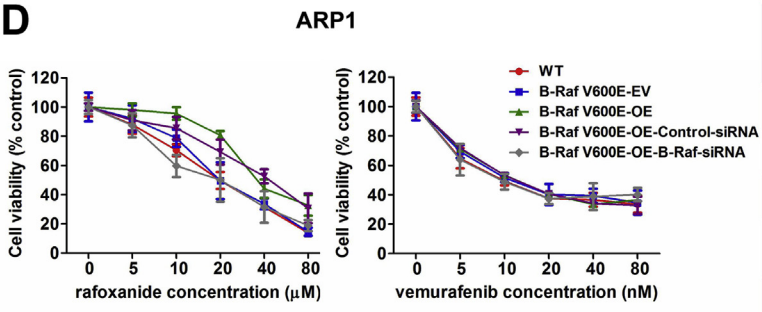

ARP1 Cell lines	rafoxanide IC_{50} (μM)	vemurafenib IC_{50} (nM)
WT	20.75	11.93
B-Raf V600E-EV	23.76	15.82
B-Raf V600E-OE	45.53	16.15
B-Raf V600E-OE-Control-siRNA	41.46	15.86
B-Raf V600E-OE-B-Raf-siRNA	20.36	12.18

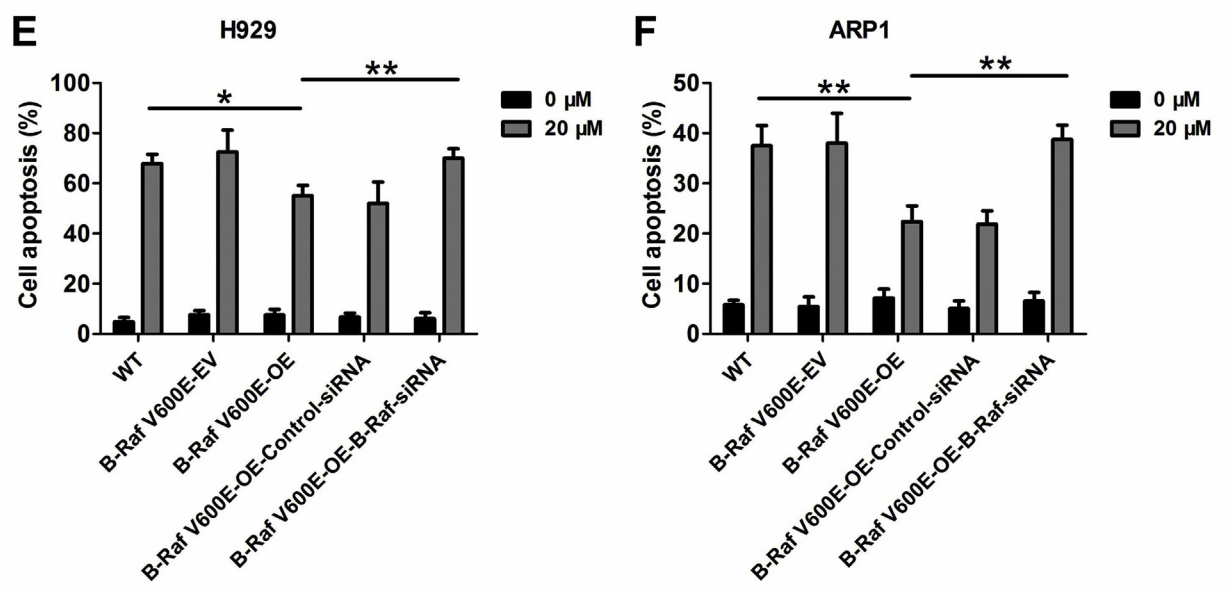

(caption on next page)

Fig. 8. Different effect of rafoxanide in wild type B-Raf, B-Raf V600E overexpressed, and B-Raf V600E knocked down MM cells. (A) Western blot analysis confirmed B-Raf V600E was effectively overexpressed after infection with B-Raf V600E overexpression (B-Raf V600E-OE) lentivirus in H929 and ARP1 cells. (B) Western blot analysis confirmed B-Raf V600E was effectively knocked down after transfection with siRNA against B-Raf gene using Lipofectamine 3000 transfection reagent in H929−B-Raf V600E-OE and ARP1-B-Raf V600E-OE cells. (C–D) MM cells were treated with rafoxanide (0, 5, 10, 20, 40, or 80 μM) or vemurafenib (0, 5, 10, 20, 40, or 80 nM) for 48 h and cell viability was analyzed using a CCK8 kit. Then IC_{50} of MM cells after rafoxanide or vemurafenib treatment was determined by using CalcuSyn software, Version 2.0. (E–F) MM cells were treated with rafoxanide (0 or 20 μM) for 48 h, and apoptosis was detected by Annexin-V/PI staining followed by flow cytometry. Data are represented as mean ± SD of three independent experiments and $*p \leq 0.05$, $**p \leq 0.01$, by unpaired two-tailed Student's t tests.

tolerated drug in MM treatment.

Combinational therapy is widely required after primary therapy in MM patients. Therefore, we detected whether rafoxanide could be enhance the cytotoxicity of anti-MM agents, such as bortezomib and lenalidomide. Our data showed that combination of rafoxanide with bortezomib or lenalidomide induced synergistic cytotoxicity in MM cells. The synergistic effect suggests that combination of rafoxanide with bortezomib or lenalidomide may be a promising therapeutic strategy in MM patients. Additionally, the in *vivo* efficacy of combination of rafoxanide and bortezomib and the main mechanism of this synergistic effect is being investigated in our laboratory.

To determine whether rafoxanide is a B-Raf V600E inhibitor, we constructed B-Raf V600E mutated MM cells *in vitro*. Unexpectedly, our data indicated that the anti-proliferation effect of rafoxanide is weaker than vemurafenib in MM cells, and the IC_{50} level of rafoxanide *in vitro* is inconsistent with our previous studies. In view of the conflicting results, further studies are necessary to investigate whether these discrepancies are due to specific experiment design, inherent MM cells performance, drug characteristic, or other factors. Nevertheless, our preliminary findings also reveal that rafoxanide has anti-MM effect on both wild type and mutated cells, and provide a theoretical basis for the therapeutic dose of rafoxanide in MM patients with or without B-Raf V600E mutation. Certainly, further studies are needed to explore other potential mechanisms and the optimal dose for future clinical attempts.

In conclusion, rafoxanide, as an anthelmintic drug, effectively exerts anti-MM activity by enhancing the DNA damage response and suppressing the p38 MAPK pathway by inhibiting MM cell proliferation, inducing MM cells apoptosis, reducing MMP, causing accumulation of MM cells in G_0G_1 phase, retarding tumor growth *in vivo*, and inducing synergistic cytotoxicity in combination with bortezomib or lenalidomide. Our study demonstrates that the potential rafoxanide in the treatment of MM. However, the detailed mechanisms of whether its therapeutic effect is related to targeting B-Raf V600E mutation in MM require further investigation.

Conflicts of interest

The authors declare no conflict of interest.

Acknowledgements

This research was supported by the National Natural Science Foundation of China (No. 81570190, 81670194, 81602515 and 81372391). We thank professor Fenghuang Zhan (Department of Internal Medicine, University of Iowa, Iowa City, IA, USA) for kind gift of ARP1, OCI-MY5, OPM2 and RPMI8226 MM cell lines, and thank professor Ping Wang (Tongji University School of Medicine, Shanghai, China) for kind gift of GFP expressing lentivirus.

Appendix A. Supplementary data

Supplementary data to this article can be found online at https://doi.org/10.1016/j.canlet.2018.12.014.

References

[1] R.A. Kyle, S.V. Rajkumar, Multiple myeloma, N. Engl. J. Med. 351 (2004) 1860–1873.
[2] R.A. Kyle, S.V. Rajkumar, Multiple myeloma, Blood 111 (2008) 2962–2972.
[3] H. Ludwig, J.S. Miguel, M.A. Dimopoulos, A. Palumbo, R. Garcia Sanz, R. Powles, S. Lentzsch, W. Ming Chen, J. Hou, A. Jurczyszyn, K. Romeril, R. Hajek, E. Terpos, K. Shimizu, D. Joshua, V. Hungria, A. Rodriguez Morales, D. Ben-Yehuda, P. Sondergeld, E. Zamagni, B. Durie, International Myeloma Working Group recommendations for global myeloma care, Leukemia 28 (2014) 981–992.
[4] S.K. Kumar, S.V. Rajkumar, A. Dispenzieri, M.Q. Lacy, S.R. Hayman, F.K. Buadi, S.R. Zeldenrust, D. Dingli, S.J. Russell, J.A. Lust, P.R. Greipp, R.A. Kyle, M.A. Gertz, Improved survival in multiple myeloma and the impact of novel therapies, Blood 111 (2008) 2516–2520.
[5] K.M. Kortum, E.K. Mai, N.H. Hanafiah, C.X. Shi, Y.X. Zhu, L. Bruins, S. Barrio, P. Jedlowski, M. Merz, J. Xu, R.A. Stewart, M. Andrulis, A. Jauch, J. Hillengass, H. Goldschmidt, P.L. Bergsagel, E. Braggio, A.K. Stewart, M.S. Raab, Targeted sequencing of refractory myeloma reveals a high incidence of mutations in CRBN and Ras pathway genes, Blood 128 (2016) 1226–1233.
[6] M. Michiels, W. Meuldermans, J. Heykants, The metabolism and fate of closantel (Flukiver) in sheep and cattle, Drug Metab. Rev. 18 (1987) 235–251.
[7] H. Van Den Bossche, H. Verhoeven, O. Vanparijs, H. Lauwers, D. Thienpont, Closantel, a new antiparasitic hydrogen ionophore [proceedings], Arch. Int. Physiol. Biochim. 87 (1979) 851–853.
[8] K. Matsubara, S. Sanoh, S. Ohta, S. Kitamura, K. Sugihara, N. Fujimoto, An improved thyroid hormone reporter assay to determine the thyroid hormone-like activity of amiodarone, bithionol, closantel and rafoxanide, Toxicol. Lett. 208 (2012) 30–35.
[9] M.A. AlAmri, H. Kadri, L.J. Alderwick, N.S. Simpkins, Y. Mehellou, Rafoxanide and closantel inhibit SPAK and OSR1 kinases by binding to a highly conserved allosteric site on their C-terminal domains, ChemMedChem 12 (2017) 639–645.
[10] M. Yurdakok, Rafanoxide therapy in a child with fascioliasis, Mikrobiyol. Bul. 19 (1985) 38–40.
[11] M. Gooyit, K.D. Janda, Reprofiled anthelmintics abate hypervirulent stationary-phase Clostridium difficile, Sci. Rep. 6 (2016) 33642.
[12] Y. Li, B. Guo, Z. Xu, B. Li, T. Cai, X. Zhang, Y. Yu, H. Wang, J. Shi, W. Zhu, Repositioning organohalogen drugs: a case study for identification of potent B-Raf V600E inhibitors via docking and bioassay, Sci. Rep. 6 (2016) 31074.
[13] E. O'Donnell, N.S. Raje, Targeting BRAF in multiple myeloma, Cancer Discov. 3 (2013) 840–842.
[14] M. Andrulis, N. Lehners, D. Capper, R. Penzel, C. Heining, J. Huellein, T. Zenz, A. von Deimling, P. Schirmacher, A.D. Ho, H. Goldschmidt, K. Neben, M.S. Raab, Targeting the BRAF V600E mutation in multiple myeloma, Cancer Discov. 3 (2013) 862–869.
[15] U.J.M. Mey, C. Renner, R. von Moos, Vemurafenib in combination with cobimetinib in relapsed and refractory extramedullary multiple myeloma harboring the BRAF V600E mutation, Hematol. Oncol. 35 (2017) 890–893.
[16] J.A. McCubrey, L.S. Steelman, W.H. Chappell, S.L. Abrams, E.W. Wong, F. Chang, B. Lehmann, D.M. Terrian, M. Milella, A. Tafuri, F. Stivala, M. Libra, J. Basecke, C. Evangelisti, A.M. Martelli, R.A. Franklin, Roles of the Raf/MEK/ERK pathway in cell growth, malignant transformation and drug resistance, Biochim. Biophys. Acta 1773 (2007) 1263–1284.
[17] H. Uchiyama, B.A. Barut, A.F. Mohrbacher, D. Chauhan, K.C. Anderson, Adhesion of human myeloma-derived cell lines to bone marrow stromal cells stimulates interleukin-6 secretion, Blood 82 (1993) 3712–3720.
[18] T. Hideshima, C. Mitsiades, G. Tonon, P.G. Richardson, K.C. Anderson, Understanding multiple myeloma pathogenesis in the bone marrow to identify new therapeutic targets, Nat. Rev. Canc. 7 (2007) 585–598.
[19] M.M. Ghoneim, M. El-Ries, A.M. Hassanein, A.M. Abd-Elaziz, Voltammetric assay of the anthelmintic veterinary drug nitroxynil in bulk form and formulation at a mercury electrode, J. Pharmaceut. Biomed. Anal. 41 (2006) 1268–1273.
[20] P.G. Richardson, C.C. Hofmeister, N.S. Raje, D.S. Siegel, S. Lonial, J. Laubach, Y.A. Efebera, D.H. Vesole, A.K. Nooka, J. Rosenblatt, D. Doss, M.H. Zaki, A. Bensmaine, J. Herring, Y. Li, L. Watkins, M.S. Chen, K.C. Anderson, Pomalidomide, bortezomib and low-dose dexamethasone in lenalidomide-refractory and proteasome inhibitor-exposed myeloma, Leukemia 31 (2017) 2695–2701.
[21] K.C. Anderson, Oncogenomics to target myeloma in the bone marrow microenvironment, Clin. Canc. Res. : Official J. Am. Assoc. Canc. Res. 17 (2011) 1225–1233.
[22] V.A. Gupta, S.M. Matulis, J.E. Conage-Pough, A.K. Nooka, J.L. Kaufman, S. Lonial, L.H. Boise, Bone marrow microenvironment-derived signals induce Mcl-1 dependence in multiple myeloma, Blood 129 (2017) 1969–1979.
[23] C.S. Bryant, S. Kumar, S. Chamala, J. Shah, J. Pal, M. Haider, S. Seward, A.M. Qazi, R. Morris, A. Semaan, M.A. Shammas, C. Steffes, R.B. Potti, M. Prasad, D.W. Weaver, R.B. Batchu, Sulforaphane induces cell cycle arrest by protecting RB-E2F-1 complex in epithelial ovarian cancer cells, Mol. Canc. 9 (2010) 47.
[24] K. Liu, T. Ren, Y. Huang, K. Sun, X. Bao, S. Wang, B. Zheng, W. Guo, Apatinib promotes autophagy and apoptosis through VEGFR2/STAT3/BCL-2 signaling in

osteosarcoma, Cell Death Dis. 8 (2017) e3015.
[25] Y. Kiraz, A. Adan, M. Kartal Yandim, Y. Baran, Major apoptotic mechanisms and genes involved in apoptosis, Tumour Biol. : J. Int. Soc. Oncodev. Biol. Med. 37 (2016) 8471–8486.
[26] B. Xie, Z. Xu, L. Hu, G. Chen, R. Wei, G. Yang, B. Li, G. Chang, X. Sun, H. Wu, Y. Zhang, B. Dai, Y. Tao, J. Shi, W. Zhu, Pterostilbene inhibits human multiple myeloma cells via ERK1/2 and JNK pathway in vitro and in vivo, Int. J. Mol. Sci. 17 (2016).
[27] G. Gorgun, E. Calabrese, T. Hideshima, J. Ecsedy, G. Perrone, M. Mani, H. Ikeda, G. Bianchi, Y. Hu, D. Cirstea, L. Santo, Y.T. Tai, S. Nahar, M. Zheng, M. Bandi, R.D. Carrasco, N. Raje, N. Munshi, P. Richardson, K.C. Anderson, A novel Aurora-A kinase inhibitor MLN8237 induces cytotoxicity and cell-cycle arrest in multiple myeloma, Blood 115 (2010) 5202–5213.
[28] K. Bhattacharya, A.K. Bag, R. Tripathi, S.K. Samanta, B.C. Pal, C. Shaha, C. Mandal, Mahanine, a novel mitochondrial complex-III inhibitor induces G0/G1 arrest through redox alteration-mediated DNA damage response and regresses glioblastoma multiforme, Am. J. Canc. Res. 4 (2014) 629–647.
[29] Z. Yuan, W. Guo, J. Yang, L. Li, M. Wang, Y. Lei, Y. Wan, X. Zhao, N. Luo, P. Cheng, X. Liu, C. Nie, Y. Peng, A. Tong, Y. Wei, PNAS-4, an early DNA damage response gene, induces S phase Arrest and apoptosis by activating checkpoint kinases in lung cancer cells, J. Biol. Chem. 290 (2015) 14927–14944.
[30] D.K. Walters, X. Wu, R.C. Tschumper, B.K. Arendt, P.M. Huddleston, K.J. Henderson, A. Dispenzieri, D.F. Jelinek, Evidence for ongoing DNA damage in multiple myeloma cells as revealed by constitutive phosphorylation of H2AX, Leukemia 25 (2011) 1344–1353.
[31] Y. Dai, S. Chen, X.Y. Pei, J.A. Almenara, L.B. Kramer, C.A. Venditti, P. Dent, S. Grant, Interruption of the Ras/MEK/ERK signaling cascade enhances Chk1 inhibitor-induced DNA damage in vitro and in vivo in human multiple myeloma cells, Blood 112 (2008) 2439–2449.
[32] O. Burmistrova, J. Quintana, J.G. Diaz, F. Estevez, Astragalin heptaacetate-induced cell death in human leukemia cells is dependent on caspases and activates the MAPK pathway, Cancer Lett. 309 (2011) 71–77.
[33] O. Surova, B. Zhivotovsky, Various modes of cell death induced by DNA damage, Oncogene 32 (2013) 3789–3797.
[34] M.H. Cobb, MAP kinase pathways, Prog. Biophys. Mol. Biol. 71 (1999) 479–500.
[35] C.S.A. Tutuka, M.C. Andrews, J.M. Mariadason, P. Ioannidis, C. Hudson, J. Cebon, A. Behren, PLX8394, a new generation BRAF inhibitor, selectively inhibits BRAF in colonic adenocarcinoma cells and prevents paradoxical MAPK pathway activation, Mol. Canc. 16 (2017) 112.